

Applications of High-Energy Synchrotron Radiation for Structural Studies of Polycrystalline Materials

H. F. Poulsen,^a S. Garbe,^a T. Lorentzen,^a D. Juul Jensen,^a F. W. Poulsen,^a N. H. Andersen,^b T. Frello,^b R. Feidenhans'l^b and H. Graafsma^c

^aMaterials Department, Risø National Laboratory, DK-4000 Roskilde, Denmark,

^bDepartment of Solid State Physics, Risø National Laboratory, DK-4000 Roskilde, Denmark, and ^cEuropean Synchrotron Radiation Facility, BP 220, F-38043 Grenoble, France. E-mail: henning.friis.poulsen@risoe.dk

(Received 24 September 1996; accepted 31 January 1997)

The large penetration power of high-energy X-rays (>60 keV) raises interesting prospects for new types of structural characterizations of polycrystalline materials. It becomes possible in a non-destructive manner to perform local studies, within the *bulk* of the material, of the fundamental materials physics properties: grain orientations, strain, dislocation densities *etc.* In favourable cases these properties may be mapped in three dimensions with a spatial resolution that matches the dimensions of the individual grains. Imbedded volumes and interfaces become accessible. Moreover, the high energies allow better *in-situ* studies of samples in complicated environments (industrial process optimization). General techniques for research in this energy range have been developed using broad-band angle-dispersive methods, on-line two-dimensional detectors and conical slits. Characterizations have been made at the level of the individual grains and grain boundaries as well as on ensembles of grains. The spatial resolution is presently of the order of 10–100 µm. Four examples of applications are presented along with an outlook.

Keywords: high-energy synchrotron radiation; texture; residual stress; Bi-2223; solid-oxide fuel-cell concept (SOFC); industrial process optimization.

1. Introduction

Dedicated beamlines for high-energy X-ray diffraction (>60 keV) have recently become available at several synchrotrons. Their use for research on single crystals and amorphous materials is now established (*cf.* Schneider *et al.*, 1994). In this report we focus on their applicability for studies of polycrystalline materials such as metals, alloys and ceramics.

High-energy X-rays are associated with a large penetration power, which makes it possible to investigate millimetre- to centimetre-sized samples. This is crucial, as polycrystalline research is often concerned with structural materials, where processing or application in general put restrictions on the sample dimensions. At the same time there may be unwanted surface effects, *e.g.* strain relaxation, corrosion, friction or atypical grain growth. The optimum X-ray energy, which is mostly a trade-off between penetration depth and photon flux, is for many applications with materials of medium atomic number, including steel, nickel, copper and various ceramics, in the range 60–100 keV.

With state-of-the-art insertion devices, such as small-gap undulators at the APS (Shastri, Dejus, Haeffner & Lang, 1995), the available flux at 100 keV may be as high as 2×10^{13} photons s⁻¹ (0.1% bandwidth)⁻¹ through a 5 × 2 mm pinhole at 30 m distance. The unique combi-

nation of flux and penetration power raises prospects for performing local studies in the bulk of materials. This is obviously interesting for applications with imbedded volumes or interfaces, *e.g.* thick multilayers. Perhaps more importantly, the minimal gauge volume may in favourable cases be comparable with or smaller than the grain size. For the first time, it therefore becomes possible to measure non-destructively the fundamental microstructural parameters related to the individual grains: crystallographic orientation, strain, size, dislocation density, as well as the topology of the grain boundaries. Predictions of the macroscopic properties of the materials, such as texture, flow stress, fatigue strength, corrosion resistance, magnetization and superconducting critical current, depend heavily on these parameters. It therefore seems likely that being able to map the microstructure in three dimensions will significantly enhance our capability of predicting the macroscopic properties.

Another important aspect of the large penetration power is the improved option for performing *in-situ* studies of samples in complicated environments. This is especially of interest for applied work (industrial process optimization). Finally, for some applications, including dislocation density measurements, it may also be of importance that the primary extinction vanishes, implying that kinematical models can be used.

The other main difference between diffraction at high energies and at conventional energies (5–20 keV) is the smaller Bragg angles. These imply that the Q -space resolution becomes worse. However, a poor resolution can often be tolerated as most samples of interest consist of (a small number of) well known phases with small unit cells. Actually, from a practical point of view, it may be more important that the smaller Bragg angles make it easier to use a two-dimensional detector, as the whole diffraction pattern can be acquired on a flat device such as an image plate or a CCD camera. The small Bragg angles also imply that the local gauge volumes tend to have a long dimension along the beam direction. In some situations this problem can be overcome by scanning the sample in the direction of the beam and defining the grain boundary as positioned at the intensity half point.

2. Experimental technique

The work presented here was performed almost exclusively on beamlines BW5 at HASYLAB and ID11 at ESRF, and with X-ray energies between 80 and 100 keV. In this section we will use the experimental configuration for determination of local texture/grain orientations, shown in Fig. 1, as an example of technique.

Texture determinations do not put high demands on angular resolution, 1–3° is normally sufficient. The energy bandpass can therefore be as broad as 1%, with the limit actually being set by geometrical demands related to how the local volume is defined (*cf.* below). So far, broad-band focusing optics have not been implemented at high-energy beamlines. At present, the experiments are therefore performed with an unfocused beam and with mosaic monochromator and analyzer crystals. Initially, we have mostly used SrTiO₃ crystals. However, experience has shown that this material has drawbacks in terms of homogeneity as well as radiation damage. A better choice

might be Si-TaSi₂ (Neumann, Schneider, Süssenbach, Stock & Rek, 1996), Cu or plastically deformed Ge.

Experiments at high energies tend to be intensity limited. Full use should therefore be made of two-dimensional detectors. Image plates and CCD cameras, coupled either to an image intensifier or to a phosphor by tapered fibre optics, can all be manufactured to have a reasonable efficiency up to 100 keV. However, stability concerns rule out the use of image intensifiers. The spatial resolution (FWHM) of commercially available devices is in all cases 100 μm or worse. We have used a modified XIOS-II camera from Photonics Science – a 12-bit tapered fibre-optics CCD with an area of 77 × 83 mm².

The poor spatial resolution of the available detectors rules out tomographic techniques, where the origin of the diffracted signal is inferred from the detector itself. Instead, the gauge volume must be defined by a cross-beam technique, where both the incoming and the outgoing beam are defined by mechanical devices (slits). For the local texture/grain orientation experiments we have used a combination of a square pinhole on the entry side and a conical slit on the exit side, *cf.* Fig. 1 (Garbe, Thomson, Graafsma, Poulsen & Juul Jensen, 1996). The conical slit is a 5 mm-thick Ta plate with two 20 μm-thick conical openings corresponding to the ⟨311⟩ and ⟨200⟩ reflections of an f.c.c. system. In addition to those shown in Fig. 1, several other slits were introduced to serve as guard slits.

The Q -space resolution of a high-energy X-ray triple-axis diffractometer has been described in detail by Rütt, Neumann, Poulsen & Schneider (1995). With perfect monochromator and analyzer crystals the longitudinal resolution, $\Delta Q_{||}$, in a dispersive set-up is simply proportional to $1/\lambda$:

$$\Delta Q_{||} = (4\pi/\lambda)\Delta_{\text{div}}|1 - (d_{M/A}/d_s)|. \quad (1)$$

Here, Δ_{div} is the divergence of the beam hitting the monochromator, d_s is the d spacing of the sample and

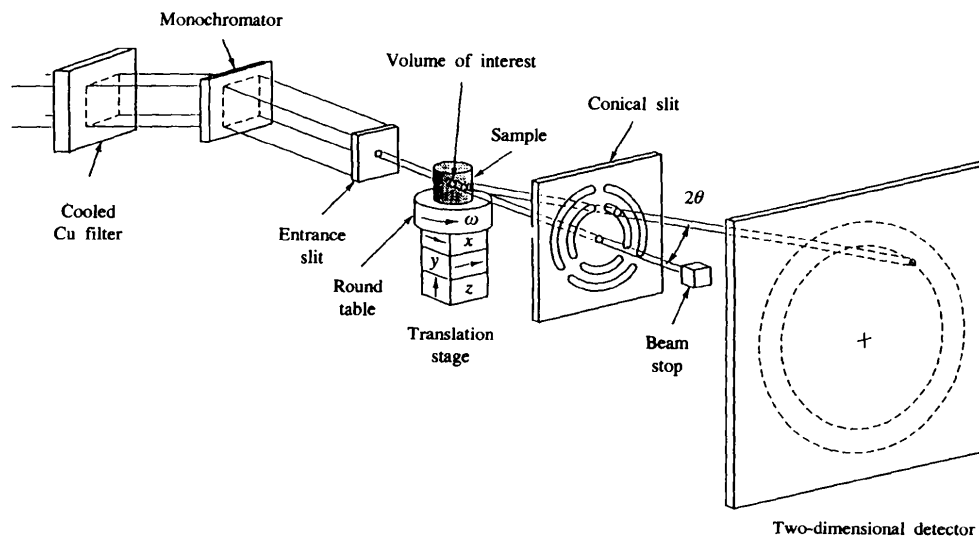


Figure 1

Experimental set-up for local texture/local grain orientation measurements. Transmission geometry is used throughout.

d_{MIA} is the common d spacing of the monochromator and analyzer. For the case of imperfect crystals, a d_s -independent term has to be added to (1). In both cases it follows that $\Delta Q_{||}$ may be improved by insertion of slits in the primary beam. The in-plane transverse resolution is for most applications, *e.g.* strain and texture determinations, much better than needed, *i.e.* of the order of minutes of arc. It may therefore be advantageous to vibrate the sample in ω during measurements. Turning next to a two-axis set-up, the direct-space contribution to the 2θ resolution tends to dominate. For fixed gauge volume and fixed sample-to-detector distance, this implies that the 2θ resolution deteriorates linearly with $1/\lambda$. The dimensions of the experimental hutches are therefore a major concern.

The obtainable spatial resolution depends drastically on Z (atomic number), sample thickness, degree of deformation and grain size.

The analysis of the two-dimensional images is simplified in the cases where the scattering from the local volume can be approximated as powder or single-grain diffraction. For the 'grey area' between these extremes, which cannot be neglected here, the available software is limited.

A texture/powder integration program, *CONE*, has been developed at Risø (Jensen, Schou, Carstensen, Poulsen & Garbe, 1996). This program deals with a set of complications that arise for the present applications. Firstly, the signal-to-noise ratio is often poor due to the simultaneous demands for fast and local measurements, and the use of complicated sample environments. The background subtraction therefore has to be based on an analysis of the local variations within the image. Secondly, it is non-trivial to parameterize the traces of the cones in the image as partial data sets are often recorded. Centre positions may therefore be unknown. Images also deviate from the ideal circular shape due to misalignments *etc.* Combined with the fact that the texture components are often rather sharp, this makes it necessary to employ image-processing methods to find the parameters of the traces. In the present case they are found by a combination of a circular Hough transform and non-linear least-squares fitting.

3. Residual strain in metal-matrix composites

The incorporation of stiff inclusions in a ductile metal is known to strengthen the metal and to improve creep properties and wear resistance. The exact strengthening mechanism in the resulting metal-matrix composite and, in particular, the influence of the mismatch in elastic/plastic behaviour of the two components, is a central issue in materials research. Experimentally, neutron diffraction has been used to determine the volume average deformations of the two constituents, while electron microscopy has given qualitative information on a local scale (results are severely influenced by the sectioning).

We have used high-energy X-rays to determine the three-dimensional strain fields around single inclusions in two model systems. Conventional 2θ scans were performed with

a scintillation counter as detector. Various strain components were successfully measured with a precision of $\Delta\varepsilon = 1 \times 10^{-4}$. The results have added new elements to our understanding of these systems. Similar types of experiment may, in the future, be used for direct tests of some of the fundamental assumptions in present-day models (*e.g.* the underlying continuum mechanics formalism).

In the first experiment (Lorentzen, Clarke, Poulsen, Garbe & Graafsma, 1997), composite cylindrical samples were produced by casting copper around a long single-fibre inclusion of tungsten. Samples were subsequently wire drawn to reduce the grain size sufficiently that measurements were essentially 'powder-like'. Eight of these samples, with varying thermal history, were characterized within 48 h of beamtime at ESRF. The gauge volume was $20 \times 100 \times 270 \mu\text{m}^3$. Most notable among the results, all samples showed evidence of large gradients in the axial strain between the sample surface and the fibre/matrix interface. These strain variations were independent of axial position even when measurements were made far from the end of the fibres. On the other hand, the radial lattice strain varied only weakly (of the order of $\pm 3 \times 10^{-4}$). As an example, the axial strain results for one of the samples are shown in Fig. 2.

Such observations are not consistent with the residual strain variations being due to thermal expansion, or plastic/elastic mismatch between the W fibre and Cu matrix. Instead we attribute them to deformations of the Cu matrix by the W fibre as the fibre slips relative to the matrix during wire drawing. This results in a uniaxial compressive stress in the core of the Cu matrix balanced by tensile stresses towards the sample surface similar to the process of inducing biaxial stresses by grinding or shot-peening.

In the second experiment (Poulsen, Lorentzen, Feidenhans'l & Liu, 1997) we investigated an analogous

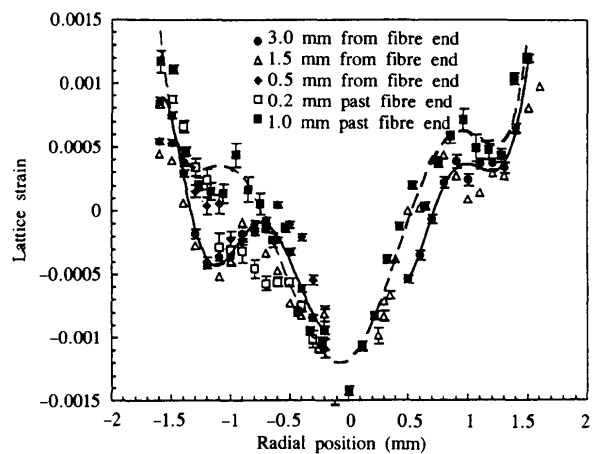


Figure 2

Cu (111) axial lattice strain as a function of radial position at several axis positions in a 3.2 mm-diameter cylindrical Cu sample with an imbedded 4.5 mm-long, 0.5 mm-diameter W fibre along the axis. The solid line is a polynomial fit to the closed circles and the dashed line is a fit to the closed squares. They are included as guides to the eye.

metal-matrix composite model system with aluminium replacing copper as the matrix material. Aluminium being lower in Z , the experiment was performed at BW2, HASYLAB, with 26 keV radiation. The gauge volume was $10 \times 10 \times 170 \mu\text{m}^3$. Two specimens were investigated with typical Al grain sizes of 1 and $30 \mu\text{m}$, respectively. In the former the intra-granular strains were mapped, *cf.* Figs. 3 and 4. In the latter the strains for individual grains with a given distance to the fibre were sampled and averaged. For both specimens we found no variation of the radial and transverse strain components with distance to the fibre,

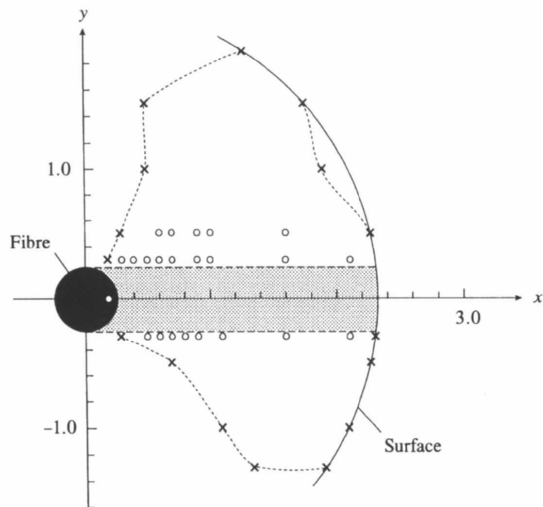


Figure 3

A sectional view through an Al/W composite with large Al grains. The crosses and dashed line mark the circumference of the grain of interest as determined by the experiment. Local strain measurements were performed at the positions marked with circles. The scattering vector was kept fixed, corresponding to the incident beam at all times being directed along the positive x axis. The shaded part of the grain was inaccessible for strain measurements with this particular scattering vector, due to absorption in the fibre.

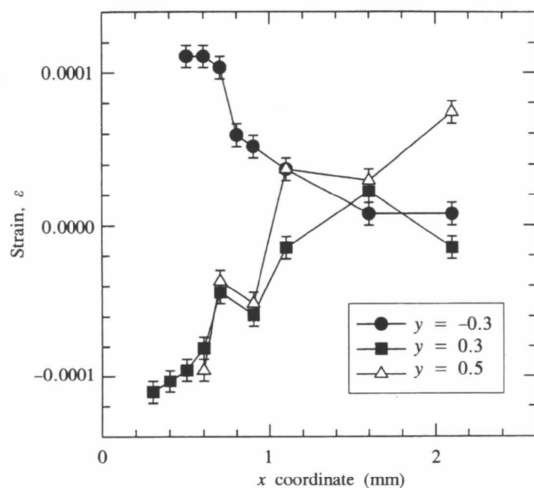


Figure 4

Strain profiles within the plane shown in Fig. 3. Error bars mark the reproducibility of the data. The intra-granular strain is seen to build up close to the grain boundary.

indicating either a complete debonding of the system or interface deterioration.

The use of two-dimensional detectors and conical slits would speed up this type of experiment, partly because 2θ scanning becomes superfluous and partly because it becomes easier to find and align the individual grains in single-grain-type experiments. However, in order to cover the full Debye-Scherrer circle with sufficient accuracy, pixel arrays of $10^4 \times 10^4$ would be needed. Also, the necessary software has, to our knowledge, not been developed.

4. Growth studies of single grains during recrystallization

The set-up shown in Fig. 1 is well suited for local texture studies. A large aluminium sample has been used as a test case (Garbe, Poulsen & Juul Jensen, 1996). The deformed

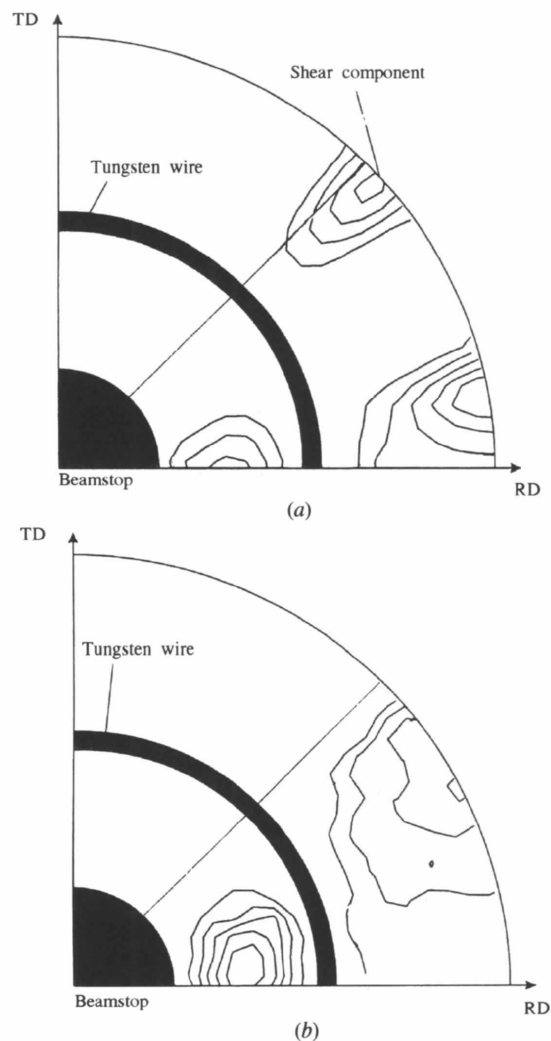


Figure 5

(200) Pole figures for two selected volumes at different depths from the surface in a deformed Al sample: (a) $d = 50 \mu\text{m}$ and (b) $d = 850 \mu\text{m}$. No information about the shaded parts was obtained due to the beam stop and W wires, used to keep the conical slit together, *cf.* Fig. 1. RD and TD denote rolling and transverse directions, respectively.

sample was annealed *in-situ* in order to follow the spatial as well as temporal evolution of the local texture. Texture components were found to change progressively with the distance to the surface of the sample. An example of resulting pole figures for the as-deformed sample is given in Fig. 5.

Our prime motivation for this type of work is to study the kinetics of recrystallization on a more local scale. The prospect of the technique is to perform *in-situ* measurements of the growth of individual grains and to correlate this growth to the texture of the surrounding deformed material. The establishment of growth laws in turn is a key ingredient for predictions of the final texture. This kind of local information cannot be achieved by other means as surface methods such as electron backscattering patterns do not give representative results. An account of a first experiment of this kind is given by Poulsen & Juul Jensen (1995).

It is also relevant to focus on the 'late-stage' regime, after complete recrystallization, where the grains start to coarsen and a characteristic topology of grain boundaries arises. To characterize a specific boundary in this network fully it is necessary to determine the crystallographic orientation of the two adjacent grains as well as the three-dimensional position of the interface. Obtaining such information, which is relevant for grain-boundary engineering purposes (Aust, 1994), is troublesome with sectioning techniques. In a feasibility study at ESRF we have partially characterized the (static) grain-boundary topology in a $4 \times 5 \times 1.4 \text{ mm}^3$ Ni sample (Garbe, Thomson *et al.*, 1996). The intensities of the reflections were mapped in two dimensions within

five sheets in the sample and with a step size of $50 \mu\text{m}$. An example of the results is given in Fig. 6. An advantage of the technique is that the accuracy of the crystallographic orientation determination can be made sufficiently small that misorientations between intra-grain cell structures can be studied.

5. *In-situ* studies of superconducting tapes

Some of the most promising applications of the high- T_c superconductors are related to the use of wires and tapes of the $(\text{Bi,Pb})_2\text{Sr}_2\text{Ca}_2\text{Cu}_3\text{O}_y$ material (abbreviated as the 2223 phase). Risø is involved in manufacturing such tapes in collaboration with other Danish institutes and the industrial partner NKT Research Centre. Precursor powder, consisting mainly of the 2212 phase $[(\text{Bi,Pb})_2\text{Sr}_2\text{Ca}_1\text{Cu}_2\text{O}_y]$, is filled into Ag tubes, which are subsequently rolled and annealed at temperatures between 1073 and 1123 K several times. During this treatment, oxygen diffuses through the Ag sheet, the 2212 phase is transformed into 2223, the superconducting grains grow and they develop a strong *c*-axis alignment. The final tapes have cross sections of approximately $3 \text{ mm} \times 200 \mu\text{m}$.

The critical current density J_c at 77 K is the crucial parameter to optimize. There seems to be ample room for substantial improvements from the state-of-the-art $J_c = 20\text{--}40 \text{ kA cm}^{-2}$, but in order to do so it may be necessary to determine exactly what happens during the thermomechanical processing, especially during the first annealing. This is complicated by the fact that conventional diffraction tools, including neutron diffraction, cannot penetrate the silver

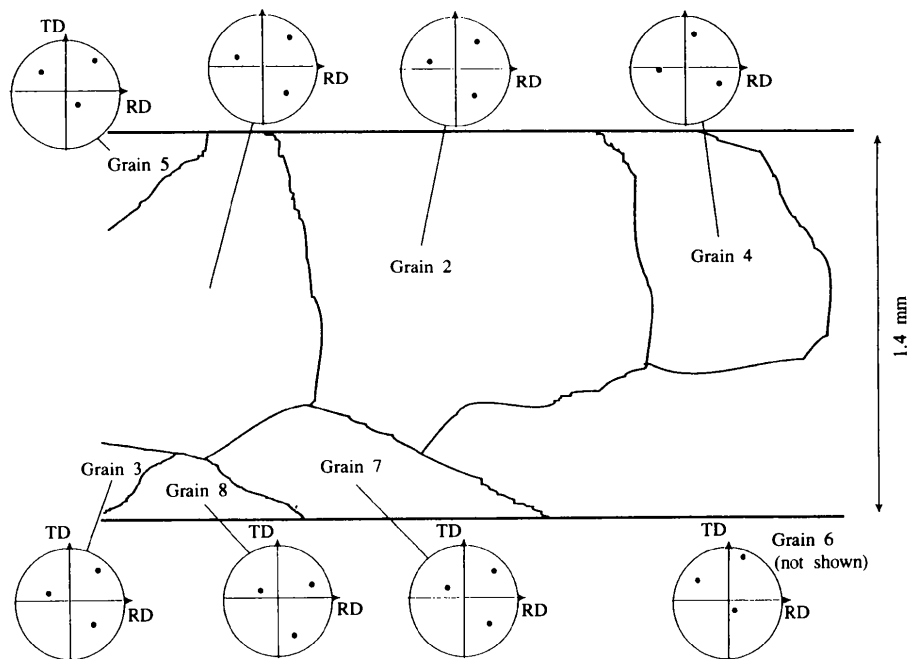


Figure 6

Slide section of eight grains in an imbedded plane in a 1.4-mm-thick Ni sample. Also shown are the determined $\langle 200 \rangle$ pole figures for the individual grains.

while on the other hand removal of the Ag sheet is known to change the results drastically.

Using 100 keV photons at HASYLAB, we have recently performed what to our knowledge are the first *in-situ* studies

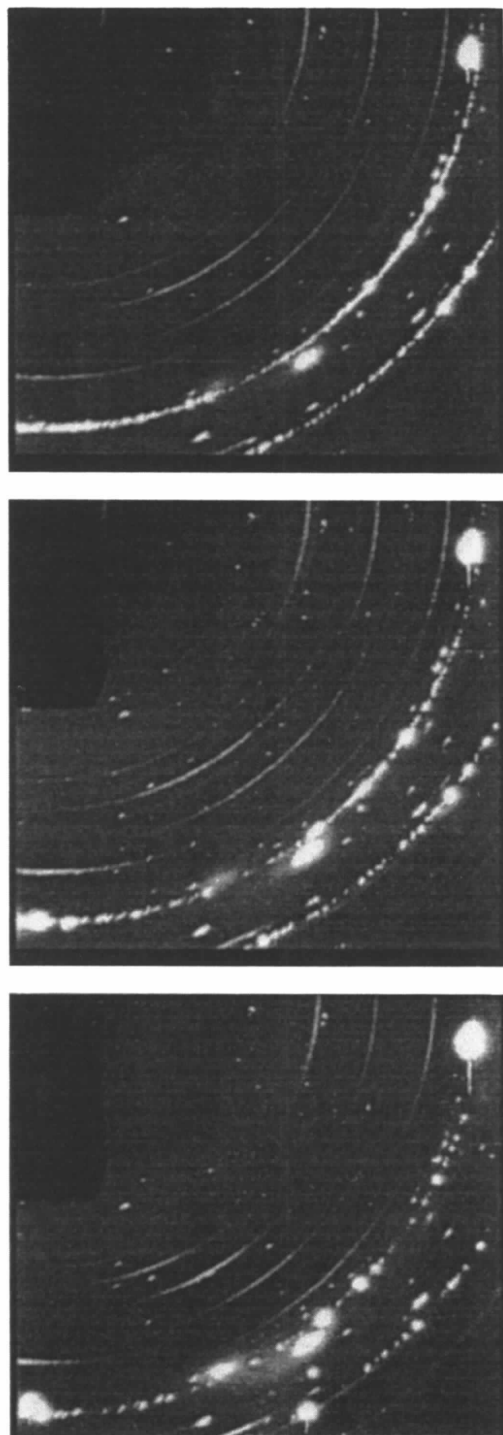


Figure 7

Exposures of a monofilament $\text{Ag}/(\text{Bi,Pb})_2\text{Sr}_2\text{Ca}_2\text{Cu}_3\text{O}_y$ superconducting tape after 0 (top), 6 (middle) and 26 h (bottom) of annealing at 1108 K. The set-up shown in Fig. 1 was used except for the conical slit (bulk data). The superconducting grains are small and give rise to smooth segments while the silver is recrystallized and gives rise to 'dotted' segments.

of the annealing process (Frello *et al.*, 1996; Poulsen, Frello *et al.*, 1996). The texture development and kinetics of the 2212 and 2223 phases, as well as some secondary phases, can clearly be followed. An example of the raw data for a multifilament tape is given in Fig. 7. The annealing process is rather slow (~ 2 d), while exposure times are ~ 1 min. The furnace was therefore designed in such a way that many tapes could be mounted in parallel and measured sequentially. This also made it possible to perform some process optimization of temperatures, oxygen partial pressures, cooling rates *etc.*

6. *In-situ* studies of fuel-cell electrodes

The solid-oxide fuel-cell concept (SOFC) is being studied intensively as a means of a more efficient and cleaner electricity-generation method, compared with conventional steam and gas-turbine technology. Cells typically consist of five layers of current collectors, electrodes and a solid-state electrolyte. They are operated at temperatures between 1050 and 1300 K. Risø National Laboratory is leading a Danish SOFC programme and an EU programme with international and local partners.

High-energy X-rays offer unique possibilities for *in-situ* characterization of fuel cells, and batteries in general, under operating conditions. In an initial study (Sörby, Poulsen, Poulsen & Garbe, 1996) we have focused on the effect of temperature and current on the structure of the 'air electrode', a 5–50 μm -thick imbedded layer of $(\text{La,Sr})\text{MnO}_{3\pm\delta}$. Under current production we find that

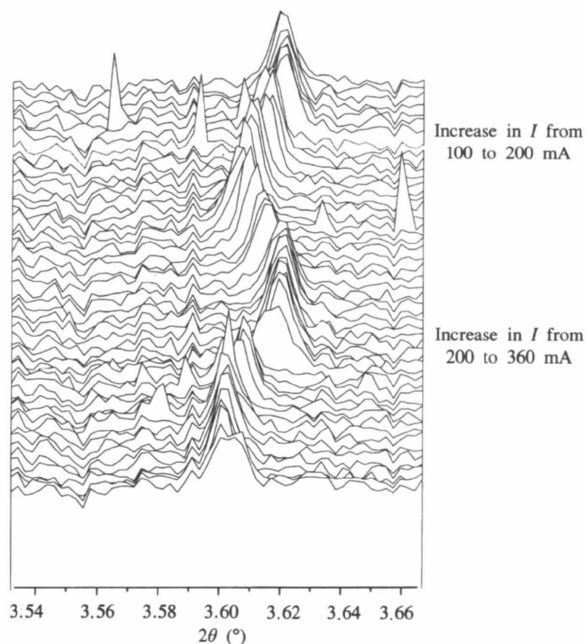


Figure 8

A close-up on the (2,0,4) $(\text{La,Sr})\text{MnO}_{3\pm\delta}$ (LSM) peak in a time-resolved set of diffractograms from polarizing an $\text{Ag}/(\text{Y,Zr})\text{O}_2/\text{LSM}$ fuel cell at 1113 K. The data were reduced to the format shown here from exposures made by a CCD camera.

the air electrode adjusts to steep gradients in oxygen potential by changing the oxygen stoichiometry (δ) leading to large reversible structural changes, *cf.* Fig. 8. This type of composition-driven structural adjustment of fuel-cell electrodes has not been reported before.

7. Outlook

From the polycrystalline research point of view the high-energy X-rays fill a gap in (spatial resolution, penetration power) space between SEM and neutron diffraction. Improving the spatial resolution is therefore a main concern. It is equally important to find better ways of measuring many local volumes in parallel, as applications tend to require the coverage of many samples as well as many local positions within each sample. We will here discuss various angle-dispersive solutions to these problems. White-beam solutions have been ruled out due to lack of suitable detectors.

The requirements to Q -space resolution are as mentioned relatively relaxed for many applications, including local strain and texture determinations as well as, in some cases, local structure identification. Broad-band focusing is therefore an option. Optic devices such as multilayers (Høghøj, 1994), Fresnel zone plates (Snigirev, 1995) and bent crystals (Suortti, Lienert & Schulze, 1994) have all been shown to give reasonable reflectivities at energies up to 100 keV. However, these devices have not yet been implemented at high energies. As a first attempt to find the optimal solution, we plan to test a combination of a bent Laue/Bragg monochromator in the horizontal and a bent multilayer in the vertical direction at ESRF. We estimate this combination will increase the flux by a factor of 50 with respect to the set-up with mosaic crystals. In the long term, a considerable flux increase may be expected from new sources, such as PETRA, the 12 GeV storage ring at Hamburg, and new insertion devices, such as small-gap undulators.

Little was done to minimize the background in the experiments presented here. Most noteworthy, a nose-piece that connects the two-dimensional detector directly to the defining slit system should be constructed. This should reduce the background significantly. From the combined effect of improvements in optics and background suppression we estimate that gauge volumes of the order of $5 \times 5 \times 50 \mu\text{m}^3$ should be within reach (best-case scenario).

With decreasing gauge volume, the machining of mechanical devices such as slits becomes a problem. Plans are to make the next generation of conical slits with the LIGA lithography technique (Bacher, Menz, Mohr, Müller & Schomburg, 1994). This also has the advantage that five or more 'rings' can be placed in one slit, allowing a full texture determination to be measured without any sample rotations. The LIGA technology can also be envisaged to have other interesting applications, such as two-dimensional Soller collimators.

Ideally, the spatial information should be extracted from the detector itself (tomography). In order to have a reasonable spatial resolution it will be necessary to incorporate high- Z material in the detector such that the photoelectric effect dominates over scattering and the diameter of the 'Compton cloud' becomes as small as possible. It is conceivable that such detectors can be manufactured in the long term. Provided a suitable detector is available, the origin of a specific signal can be traced by translating the detector forwards and backwards in the direction of the beam. The 'track' of the ray will then be estimated in much the same way as is done in high-energy physics using three-dimensional detectors. Small translation scans of the detector may also serve as a general way of improving the accuracy by which the centre of a given signal can be determined. This 'trick' may actually be sufficient to circumvent some of the previously mentioned problems of using two-dimensional detectors for strain measurements.

The ultimate microfocus set-up would be a close analogue to the SEM. Hence, it would be natural to combine microdiffraction with high-resolution high-energy imaging, an interesting undeveloped field in itself (the direct equivalent to industrial radiography).

Turning next to other applications of high-energy X-rays for materials research, we note that the local volumes are already sufficiently small that thick multilayers may be characterized by entering the beam from the side of the multilayer. A pilot experiment at BW5, HASYLAB, has shown that the intensity is sufficient for determining the strain profile in a Cu/Ni multilayer with a layer thickness of $10 \mu\text{m}$. High-energy X-rays may also be of interest for determining dislocation densities and in general for studies of peak profiles. Individual bulk grains can be studied, which clearly helps when performing diffuse studies. As mentioned, it may also be significant that the kinematic approximation will nearly always be valid. In this case, of course, broad-band focusing is not an option.

Finally, time-resolved studies are an interesting alternative. Millisecond sampling of bulk data is likely to be of importance *e.g.* for studies of stress relaxation after thermal shocks.

The authors would like to thank J. R. Schneider and the staff at beamline BW5, HASYLAB, for continuous help and encouragement. We are grateful to U. Lienert, P. Klimanek and A. Horsewell for fruitful discussions related to optics, dislocation densities and strain measurements on multilayers, respectively. Moreover, we are much indebted to A. Abrahamsen, Y. L. Liu, A. P. Clarke, P. Olesen, C. Klitholm, M. D. Bentzon, L. Sörby, C. Thomson, J. Süssenbach, D. Novikov and M. von Zimmermann for help with sample preparation and synchrotron experiments. Support for this work was provided by the Danish Research Councils through the Engineering Science Centre at Risø and through DanSync, by the Danish Energy Agency and by the companies NKT Research Centre, ELSAM and ELKRAFT.

References

- Aust, K. T. (1994). *Can. Metall. Q.* **33**(4), 265–274.
- Bacher, W., Menz, W., Mohr, J., Müller, C. & Schomburg, W. K. (1994). *Naturwissenschaften*, **81**(12), 536–545.
- Frello, T., Poulsen, H. F., Bentzon, M. D., Garbe, S., von Zimmermann, M., Abrahamsen, A. & Andersen, N. H. (1996). Unpublished.
- Garbe, S., Poulsen, H. F. & Juul Jensen, D. (1996). *Proc. ICOTOM 11; 11th Int. Conf. Text. Mater.* Xian, China.
- Garbe, S., Thomson, C., Graafsma, H., Poulsen, H. F. & Juul Jensen, D. (1996). Preprint available.
- Høghøj, P. (1994). PhD thesis, Niels Bohr Institute, University of Copenhagen, Denmark. ISSN 0906-0286-1994-03.
- Jensen, R. F., Schou, J., Carstensen, M., Poulsen, H. F. & Garbe, S. (1996). Preprint available.
- Lorentzen, T., Clarke, A. P., Poulsen, H. F., Garbe, S. & Graafsma, H. (1997). *Composites A*. In the press.
- Neumann, H.-B., Schneider, J. R., Süßenbach, J., Stock, S. R. & Rek, Z. U. (1996). *Nucl. Instrum. Methods*, **A372**(3), 551–555.
- Poulsen, H. F., Frello, T., Bentzon, M. D., Garbe, S., Novikov, D. & Andersen, N. H. (1996). Preprint available.
- Poulsen, H. F. & Juul Jensen, D. (1995). *Proc. 16th Risø Int. Symp. Mater. Sci.*, edited by N. Hansen, D. Juul Jensen, Y. L. Liu & B. Ralph. Risø National Laboratory, Roskilde, Denmark.
- Poulsen, H. F., Lorentzen, T., Feidenhans'l, R. & Liu, Y. L. (1997). *Metall. Mater. Trans. A*. In the press.
- Rütt, U., Neumann, H.-B., Poulsen, H. F. & Schneider, J. R. (1995). *J. Appl. Cryst.* **28**, 729–737.
- Schneider, J. R., Bouchard, R., Brückel, T., Lippert, M., Neumann, H.-B., Poulsen, H. F., Schmidt, T. & von Zimmermann, M. (1994). *Proc. Eur. Symp. Front. Sci. Technol. Synchrotron Rad.* Aix-en-Provence.
- Shastri, S. D., Dejus, R. J., Haeffner, D. R. & Lang, J. C. (1995). *Rev. Sci. Instrum.* **66**(9), 1–3.
- Snigirev, A. (1995). *Rev. Sci. Instrum.* **66**, 2053–2058.
- Sörby, L., Poulsen, F. W., Poulsen, H. F. & Garbe, S. (1996). Unpublished.
- Suortti, P., Lienert, U. & Schulze, C. (1994). *Nucl. Instrum. Methods*, **A338**, 27–32.